

6

Single-interface surface plasmons

Tables

Item	Topic	Chapter 3	Chapter 4	Chapter 5	Chapter 6	Chapter 7
1	Interfaces	1	1	2	1	2
2	Types	ENG, DNG	DPS, ENG, DNG, MNG	DPS, ENG, DNG, MNG	ENG	ENG
3	ϵ_r, μ_r	complex	real	real	complex	complex
4	Dispersion	yes	no	no	no	no
5	Free β	yes	yes	yes	yes	yes
6	Loaded β	yes	no	no	yes	yes
7	Configuration	O, K	free	free	O, K	G
8	\mathcal{R}	yes	no	no	yes	yes
9	G-H	yes	no	no	no	no
10	E and H	no	yes	yes	yes	yes
11	s_z	no	yes	yes	yes	yes
12	s_x	no	no	no	yes	yes
13	η	yes	no	no	yes	yes
14	v_{ph} and v_{group}	yes	no	no	no	no
15	Charge density	no	no	no	yes	yes

Table 2.10. List of topics investigated in chapters 3-7.

Item	Topic	Chapter 6
1	Interfaces	1
2	Types	ENG
3	ϵ_r, μ_r	complex
4	Dispersion	no
5	Free β	yes
6	Loaded β	yes
7	Configuration	O, K
8	\mathcal{R}	yes
9	G-H	no
10	E and H	yes
11	s_z	yes
12	s_x	yes
13	η	yes
14	v_{ph} and v_{group}	no
15	Charge density	yes

Table 6.1. List of topics investigated in this chapter.

	ϵ_i	μ_i	n_i	r_i	ϕ_i
Prism	6.25	1.	2.5		
Cover	2.25	1.	1.5	2.46221	0.418224
Silver	$-15.9958 + 0.52 i$	1.	$0.0649999 + 4. i$	16.027	3.07916
Substrate	2.25	1.	1.5	2.46221	0.418224

Table 6.2. The values of ϵ_i , μ_i , n_i , r_i and ϕ_i for the prism, cover, silver and substrate. Note that the refractive indices of the cover for the Otto configuration and the substrate for the Kretschmann configuration are composed of identical media.

β	$1.61796 + 0.00429942 i$
δ	$0.606547 + 0.0114687 i$
γ	$4.31474 - 0.0586463 i$

Table 6.3. The propagation constant, β , and the decay constants in the cover and metal, δ and γ , respectively using the parameters given in Table 2.2.

	System	ζ (μm)	N_ζ (cycles)	τ_ζ (fs)
(a) PW	silver	0.0251783	0.00258626	0.00545907
(b) SP	glass/silver	23.4248	59.8931	126.422
(c) SP	air/silver	90.0693	146.998	486.097

Table 6.4. The $1/e$ propagation distance, ζ , the number of wave cycles per decay length, N_ζ , and the lifetime, τ_ζ , for a plane wave (PW) incident normal to a thick silver film, and for SPs propagating along air/silver and glass/silver interfaces.

	η_i/η_0	$\eta_{SP,i}/\eta_0$
Cover	0.666667	$0.719092 + 0.00191085 i$
Metal	$0.00406142 - 0.249934 i$	$-0.101033 - 0.00355323 i$

Table 6.5. The relative wave impedances for a bulk dielectric and a bulk metal, η_i/η_0 , and for the surface plasmon, $\eta_{SP,i}/\eta_0$. Note that the wave impedance in all cases is mostly real, and that for the cover and the metal the impedance is positive and negative, respectively.

$P_{m,z}$	$P_{c,z}$	P_z
-0.020149	1.02014	1

Table 6.6. The total power flow in the metal and cover, $P_{c,z}$ and $P_{m,z}$, respectively, and their sum, P_z .

	E (10^3 V/m)	$ E $ (10^3 V/m)	θ_E (deg)
E_x	$-11.4636 - 0.403168 i$	11.4707	-177.986
E_z	$0.578361 - 30.587 i$	30.5925	-88.9167

Table 6.7. The complex-valued electric fields E_x and E_z at the metal-cover interface namely at $x = 0^-$, and their respective absolute value, $|E|$, and angle, θ_E , derived from the ratio of their imaginary and real parts.

β	θ_p (deg)	Γ_p (deg)
$1.61796 + 0.00429942 i$	40.3294	0.129255

Table 6.8. The complex propagating constant of the SP, β , together with its ideal Lorentzian centered at an angle of incidence of the beam in the prism, θ_p , and its respective width, Γ_p .

Figures

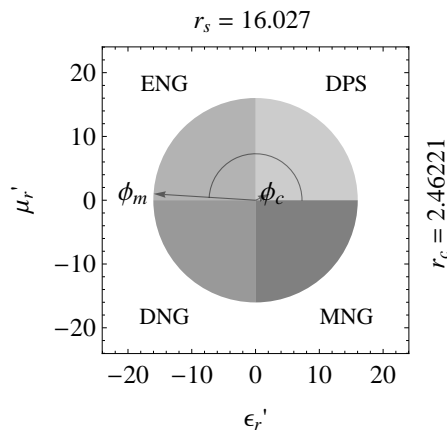


Fig. 6.3. Configuration of the DPS/ENG-type structure in an ϵ_r' - μ_r' parameter space using the parameters of Table 6.2. Note that the vectors associated with the cover and metal, that differ in their lengths and angles, are in the DPS and ENG quadrants, respectively.

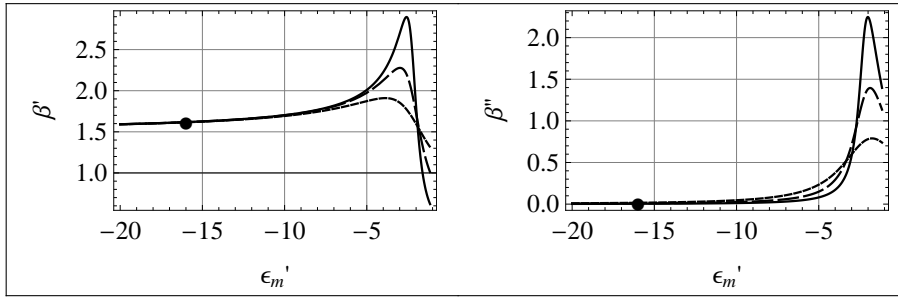


Fig. 6.4. The real (left) and imaginary (right) parts of the propagation constant, β' and β'' , respectively, as a function of ϵ_m' for $\epsilon_m'' = 0.5$ (solid line), 1 (dashed line) and 2 (dotted line).

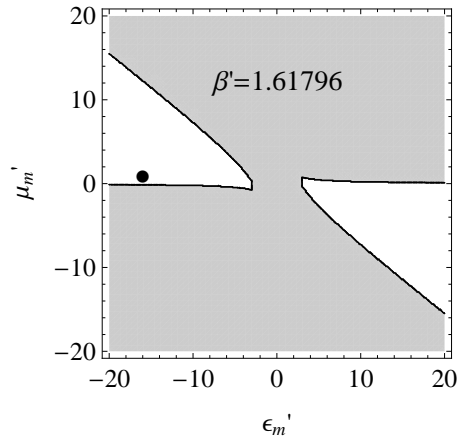


Fig. 6.5. The regions for which a DPS-ENG system can support TM modes are depicted in an ϵ_r' - μ_r' parameter space in white on a gray background. Also shown is the value of β' where the solid dot represents the value of ϵ_m' and μ_m' given in Table 6.2.

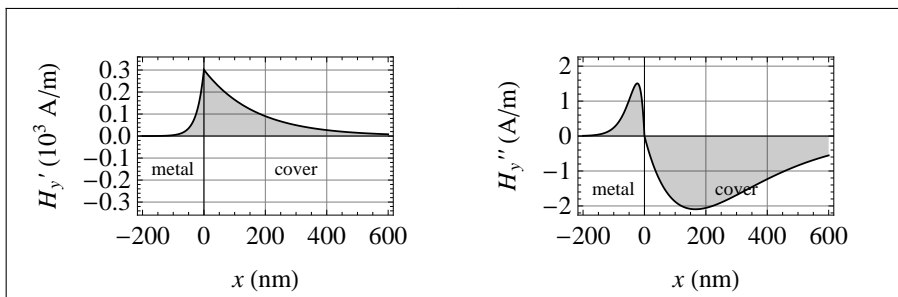


Fig. 6.6. The real (left) and imaginary (right) parts of the magnetic field of the SP, H_y' and H_y'' , respectively, as a function of position, x , normal to the metal-cover interface.

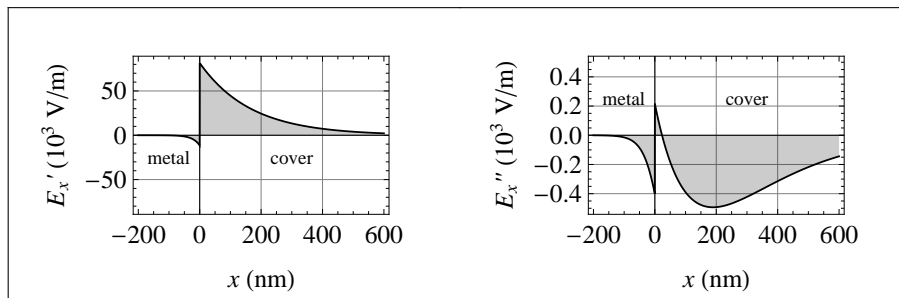


Fig. 6.7. The real (left) and imaginary (right) parts of the electric field of the SP, E_x' and E_x'' , respectively as a function of position, x , normal to the metal-cover interface.

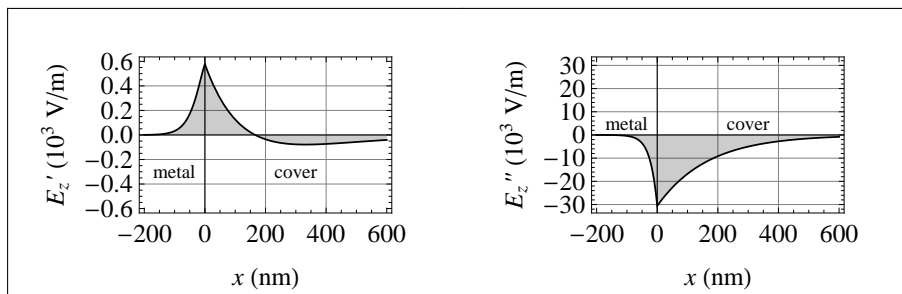


Fig. 6.8. The real (left) and imaginary (right) parts of the electric field of the SP, E_z' and E_z'' , respectively, as a function of position, x , normal to the metal-cover interface.

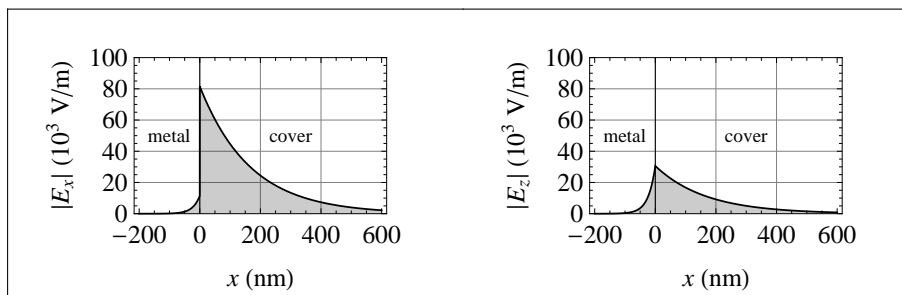


Fig. 6.9. The absolute value of the electric fields of the SP, $|E_x|$ and $|E_z|$, as a function of position, x , normal to the metal-cover interface.

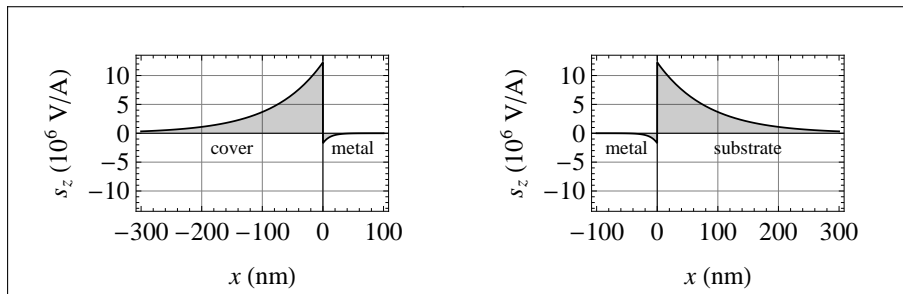


Fig. 6.11. The local power flow associated with the cover-metal (left for the Otto configuration) and metal-cover (right for the Kretschmann configuration) cases, s_z , as a function of position, x , normal to the metal-dielectric interface.

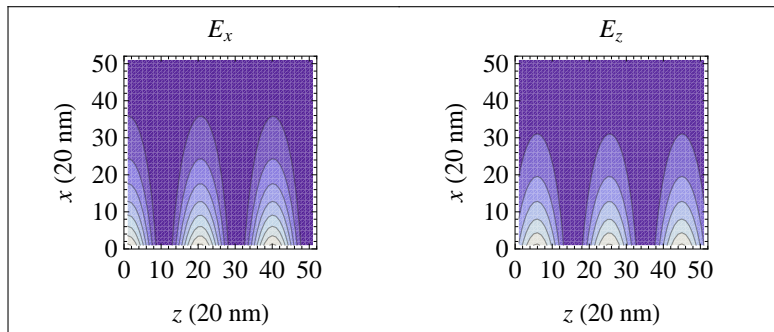


Fig. 6.12. A contour plot of the fields $E_x(x,z)$ (left) and $E_z(x,z)$ (right) in the cover as phasors, represented in terms of their magnitude and relative phase as a function of x and z which are in units of 20 nm.

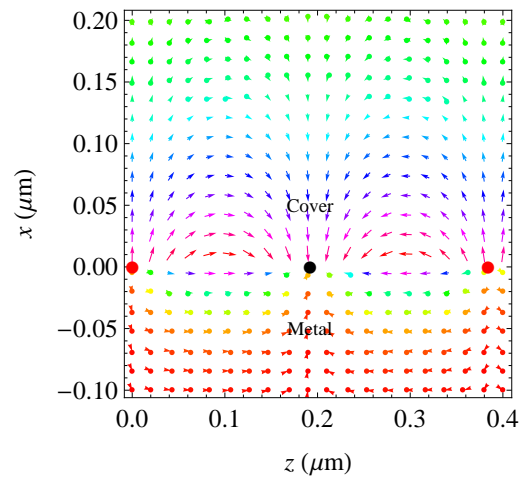


Fig. 6.13. The vector field $\mathbf{E} = \hat{x}E_x + \hat{y}E_z$ as a function of position x in the cover and metal and z along the interface, in arbitrary units.

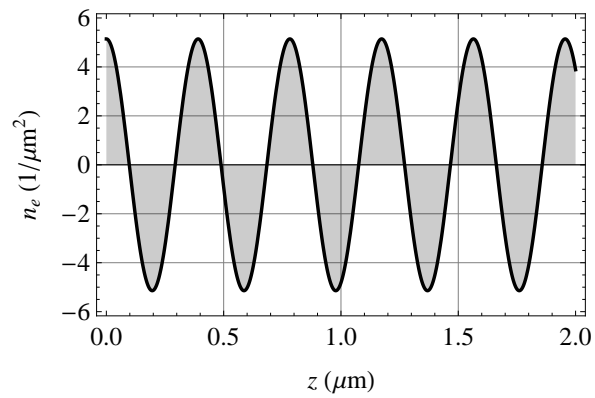


Fig. 6.14. The surface charge density wave in terms of the number of charges, n_e , at the bottom side of the cover-metal interface at $x = 0^-$.

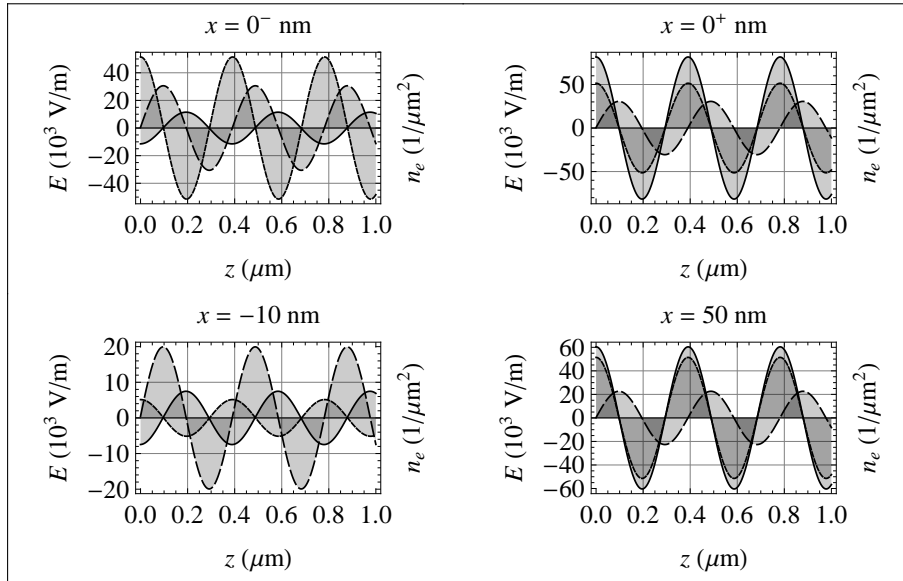


Fig. 6.15. The propagating electric fields E_x (solid line) and E_z (dashed line) and surface charge density wave in terms of n_e (dotted line) as phasors at the cover-metal interface as a function of position, z , along the propagation direction. The fields in these figures are calculated at $x = 0^-$ (top left), $x = 0^+$ (top right), $x = -10 \text{ nm}$ (bottom left) and $x = 50 \text{ nm}$ (bottom right).

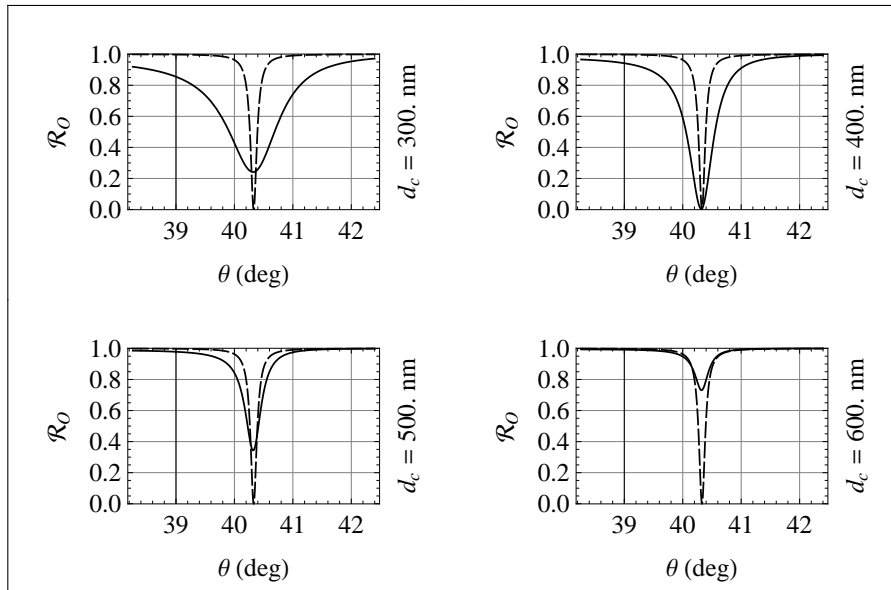


Fig. 6.17. The \mathcal{L} - and \mathcal{R}_O -spectra, depicted by the dashed and solid lines, respectively, for the Otto configuration and for $d_c = 300, 400, 500,$ and 600 nm. At around $d_c = 600$ nm, the angular position of the minimum of these two spectra and their width are quite close.

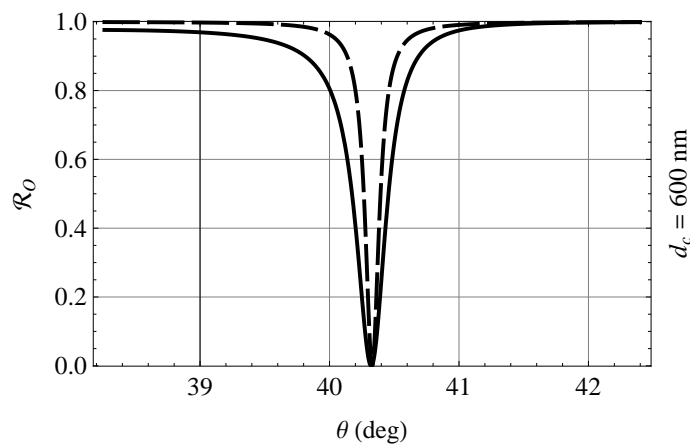


Fig. 6.18. The \mathcal{L} - and \mathcal{R}_O -spectra, depicted by the dashed and solid lines, respectively, for the Otto configuration and for $d_c = 600$ nm, showing that the spectra give a only an approximate fit for angles below and above resonance because the loading of the prism broadens the spectrum of the reflectivity.

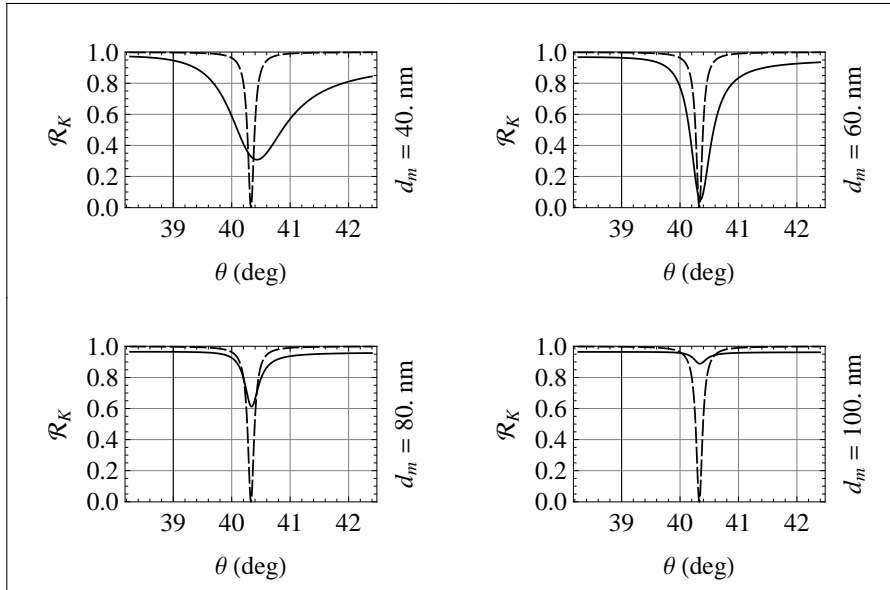


Fig. 6.20. The \mathcal{L} - and \mathcal{R}_K -spectra, depicted by the dashed and solid lines, respectively, for the Kretschmann configuration and for $d_m = 40, 60, 80,$ and 100 nm. At around $d_m = 100$ nm, the angular position of the minimum and width of the two are quite close. The dip in the reflectivity, however, is much smaller.

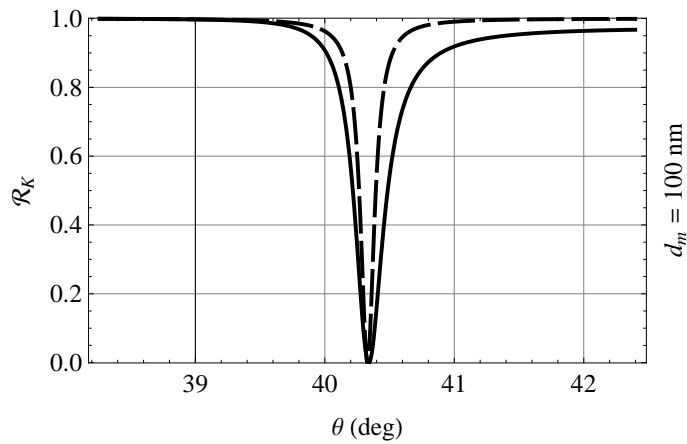


Fig. 6.21. The \mathcal{L} - and \mathcal{R}_K -spectra, depicted by the dashed and solid lines, respectively, for the Kretschmann configuration and for $d_m = 100$ nm. The fit to the ideal Lorentzian is good for angles below resonance, while above resonance the agreement is worse due to the loading of the prism.

Exercises

- (1) Complete the missing items in Table 6.1 by developing the code, generating figures and discuss them.
- (2) Compare the advantages and disadvantages of using the Otto and Kretschmann configurations.

References

- [1] H. Raether. *Excitation of Plasmons and Interband Transitions by Electrons* (Springer Tracts in Modern Physics, Vol. 88, Berlin Heidelberg New York, Springer-Verlag, 1980).
- [2] V. M. Agranovich and D. L. Mills, Eds. *Surface Polaritons, Electromagnetic Waves at Surfaces and Interfaces* (New York, North Holland, 1982).
- [3] A. D. Boardman, Ed. *Electromagnetic Surface Modes* (New York, John Wiley & Sons, 1982).
- [4] H. Raether. *Surface Plasmons on Smooth and Rough Surfaces and on Gratings* (Springer Tracts in Modern Physics, Vol. 111, New York, Springer-Verlag, 1988).
- [5] J. Pendry. Manipulating the near field with metamaterials. *OPN* 15 (2004) 32.
- [6] W. Ebbesen, C. Genet and S. I. Bozhevolnyi. Surface-plasmon circuitry. *Phys. Today* 61 (2008) 44.